Journal of Electrical Bioimpedance
www.bioimpedance.net

J Electr Bioimp, vol. 3, pp. 51–60, 2012
Received: 6 Sep 2012, published: 22 Oct 2012
doi:10.5617/jeb.400

Estimating electrical properties and the thickness of skin with electrical impedance spectroscopy: Mathematical analysis and measurements

U. Birgersson[1,3], E. Birgersson[2] and S. Ollmar[1]

1. *Department of Clinical Science, Intervention and Technology, Karolinska Institutet, SE-14186 Stockholm Sweden*
2. *Department of Chemical and Biomolecular Engineering, National University of Singapore, 5 Engineering Drive 2, Singapore 117576*
3. *E-mail: ulrik.birgersson@ki.se*

Abstract

Electrical impedance spectroscopy (EIS) allows for the study and characterization of tissue alterations and properties associated with the skin. Here, the potential application of EIS to estimate the thickness of the stratum corneum is explored in the form of a mathematical model for EIS, which is analyzed in the limit of 1 kHz and closed-form analytical solutions derived. These analytical expressions are verified with the numerical solution of the full set of equations and validated with an EIS study comprising 120 subjects: overall, good agreement is found in the frequency range 1-100 kHz, where the impedance is governed by the stratum corneum. Combining the closed-form expression for the thickness of the stratum corneum predicted by the model with the experimental EIS measurements, a distribution for the stratum corneum thickness of the subjects is found with a mean and standard deviation that agree well with reported stratum corneum thicknesses from other experimental techniques. This, in turn, suggests that EIS could be employed to measure the thickness of the stratum corneum with reasonable accuracy. In addition, the electrical properties relevant to EIS – conductivity and relative permittivity – of the stratum corneum can be estimated with the closed form expressions if the stratum corneum thickness is known.

Keywords: Dermis, electrical impedance, epidermis, mathematical model, stratum corneum

Introduction

The human skin is essentially composed of three layers – stratum corneum, living epidermis and dermis – that fulfill a range of important functions, such as acting as a mechanical and chemical barrier against the environment and upholding homeostasis by regulating water loss. The thickness of each layer varies naturally between and within individuals due to a number of biological and environmental factors: e.g., age, body site, season, race, humidity, diurnal cycle, and health condition.

It is not straightforward to measure the skin thickness and its properties in vivo due to the diverse functions of the skin and the factors affecting the skin condition. To date, a range of different techniques – confocal Raman spectrometer [1], optical coherence tomography [2], reflectance confocal microscopy [3], ultrasound imaging [4], biopsy [5] and transepidermal water loss in combination with stratum corneum stripping [6, 7] – have been employed to determine the thickness of skin with findings that often vary from one method to another. The situation is exacerbated when attempts are made to measure the thickness of the outermost layer, the stratum corneum, because of its composition and thickness in the order of 10 μm (except for the palm of the hand and foot where the stratum corneum is around ten times thicker).

In light of the difficulties associated with measuring the thickness of the stratum corneum, we aim to (*i*) explore electrical impedance spectroscopy (EIS) as an alternative technique for estimating the stratum corneum thickness, (*ii*) derive closed-form analytical solutions for our earlier mathematical model of EIS [8] that can provide a deeper understanding of the underlying phenomena and coupling of parameters than numerical simulations alone and aid in estimating the thickness of the stratum corneum, (*iii*) verify the analytical solutions with the full model and validate both with further experimental measurements, and (*iv*) estimate the stratum corneum thickness and its associated electrical properties that are key for EIS. In this context, our earlier model provides a good starting point due to its relative simplicity; it could be extended to encompass a higher resolution of the tissue with information of cellular structures from, e.g., [9–14].

In short, EIS measurements carried out with a SciBase II impedance spectrometer and a non-invasive probe [15] on skin are combined with an earlier derived mathematical model [8], for which closed-form analytical solutions are found in the limit of low frequencies around 1 kHz. We expect, based on the "forgiving" nature of approximations and leading-order solutions, that the solutions will be valid in a significant region around 1 kHz. The analytical solutions are then employed in conjunction with impedance measurements to determine the stratum corneum thickness and electrical material properties. Furthermore, in order to ensure the fidelity of the analytical expressions and establish their region of validity in the frequency spectra, verification with the numerical solution of the full set of equations is carried out; further validation with impedance measurements at different depth settings demonstrates the accuracy of the underlying mathematical model in the entire frequency spectra, $1 - 10^3$ kHz, for the SciBase II impedance spectrometer and non-invasive probe.

Materials and methods

The experimental EIS measurements are taken from a study that was carried out after ethics approval and informed consent had been obtained.

Subjects

A total of 120 young volunteers – non-smokers without any known skin diseases or allergies – participated with an equal distribution of men and women at 24 ± 3 years of age; on the day of the measurements they were asked to abstain from moisturizers.

Measurements

Electrical impedance measurements were performed on the volar forearm of the volunteers in 2007 with a SciBase II impedance spectrometer and a non-invasive probe [15].

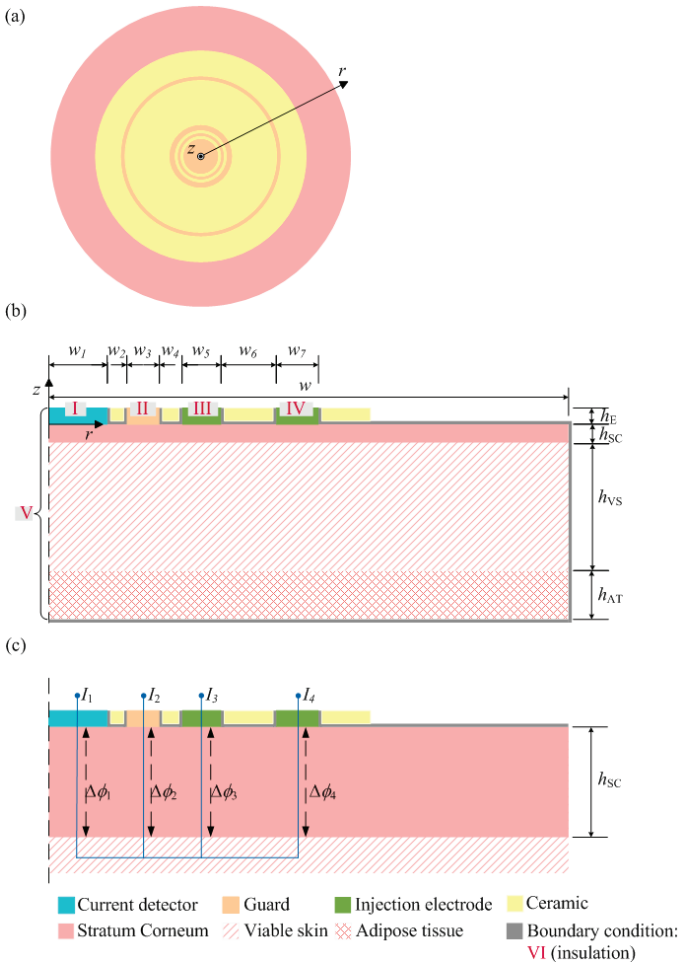

Fig. 1: Schematic overview of the non-invasive electrode applied on (a-b) stratum corneum, viable skin and adipose tissue and (c) details of the mathematical Ansatz. The boundary conditions are denoted with roman numerals. Dimensions are given in Table 1.

The non-invasive, circular probe comprises four electrodes as illustrated in Fig. 1: two voltage injection electrodes, one current detector and one guard electrode to decrease the impact of surface leakage currents. With this design, two-point measurements can be carried out. The dimensions of the electrode and the skin layers depicted in Fig. 1 can be found in Table 1.

Model object	Acronym	Dimensions
Current detection	w_1	1 mm
Ceramic	w_2, w_4, w_6	0.15, 0.15, 1.9 mm
Guard ring	w_3	0.3 mm
Secondary inject	w_5	0.5 mm
Primary inject	w_7	0.5 mm
Total width for domain	w	20 mm
Electrode thickness	h_{E}	0.1 mm
Stratum corneum thickness	h_{SC}	14 μm
Viable skin thickness	h_{VS}	1.2 mm
Adipose tissue thickness	h_{AT}	1.2 mm

Tab. 1: Dimensions for the electrode and skin layers [8].

The SciBase II impedance spectrometer measures the impedance of the skin at 35 frequencies logarithmically distributed between 1.0 kHz and 2.5 MHz at five different depth settings; these are obtained by varying the applied voltage at the second injection electrode (boundary III in Fig. 1b) from 5 to 50 mV [16].

Before measurements, the skin of the subjects was inundated with a physiological saline solution of 0.9% sodium chloride mass concentration for 1 min. The relative air humidity was 36 ± 7 %, and the ambient temperature was maintained at 21.7 ± 0.3 C.

Mathematical model

A mathematical model based on conservation of charge in both the time- and frequency-domain for an alternating, sinusoidal current in the rotation-symmetric gold-plated electrodes (EL) of the probe and the skin – stratum corneum (SC), viable skin (VS) and adipose tissue (AT) – in the vicinity of the probe was derived in our earlier work [8]. In short, the model can be expressed as follows in the frequency domain:

$$\nabla \cdot \mathbf{J} = 0, \tag{1a}$$

$$\mathbf{J} = -(\sigma^{(i)} + j\omega\varepsilon_0\varepsilon_r^{(i)})\nabla\phi, \tag{1b}$$

$$\phi(I,II) = 0, \tag{1c}$$

$$\phi(III) = \alpha V_0, \tag{1d}$$

$$\phi(IV) = V_0, \tag{1e}$$

$$\mathbf{n} \cdot \mathbf{J}(V,VI) = 0. \tag{1f}$$

Here, $\mathbf{J}$ is the total current density, $\sigma^{(i)}$and $\varepsilon_r^{(i)}$ are the conductivity and relative permittivity of layer i $(= \mathrm{SC}, \mathrm{VS}, \mathrm{AT}, \mathrm{EL})$, ϕ is the potential, α is a coefficient for a given depth setting of the second injection electrode, V_0 is the excitation voltage, j is the imaginary number, and ω is the angular frequency of the alternating current; the roman numerals denote the respective boundaries, which are highlighted in Fig. 1b.

The material properties are given by [17]:

$$\rho^{(i)}(\Omega) = 10^{(\mathfrak{c}_5^{(i)}\Omega^5+\mathfrak{c}_4^{(i)}\Omega^4+\mathfrak{c}_3^{(i)}\Omega^3+\mathfrak{c}_2^{(i)}\Omega^2+\mathfrak{c}_1^{(i)}\Omega+\mathfrak{c}_0^{(i)})}, \quad (1g)$$

$$\varepsilon_r^{(i)}(\Omega) = 10^{(\mathfrak{d}_5^{(i)}\Omega^5+\mathfrak{d}_4^{(i)}\Omega^4+\mathfrak{d}_3^{(i)}\Omega^3+\mathfrak{d}_2^{(i)}\Omega^2+\mathfrak{d}_1^{(i)}\Omega+\mathfrak{d}_0^{(i)})}, \quad (1h)$$

$$\Omega = \log_{10}(\nu), \quad (1i)$$

where i denotes either viable skin, stratum corneum soaked with a saline solution with 0.9% NaCl for 1 min, and adipose tissue (relative permittivity); ρ is the resistivity; ν is the frequency; $\mathfrak{c}_j^{(i)}$ and $\mathfrak{d}_j^{(i)}$ are the material coefficients, given in table 2. These constitutive relations for the electrical material properties are valid between 1 kHz and 1 MHz. (*N.B.*: the dependent variable, ϕ, is a phasor; for more information, see our earlier work [8].)

Scaling analysis

In our search for closed-form analytical solutions that could allow for estimates of the stratum corneum thickness and its electrical properties, we start by noting the well-known fact that the impedance is dominated by the stratum corneum at low frequencies around 1 kHz [18, 19], which suggests that the potential drop in the viable skin and electrodes are negligible vis-à-vis the corresponding drop in the stratum corneum around this frequency. This is indeed the case, as can be shown with the following scaling analysis for the potential drops in the various skin layers and electrodes: the potential drops can be secured from an order-of-magnitude equivalent of the total current density, Eq. 1b, in each layer as

$$\frac{[I]}{[A_{\mathrm{SC}}]} \sim \left|\sigma^{(\mathrm{SC})} + j\omega\varepsilon_0\varepsilon_r^{(\mathrm{SC})}\right| \frac{[\Delta\phi_{\mathrm{SC}}]}{l_{\mathrm{SC}}}, \quad (2a)$$

$$\frac{[I]}{[A_{\mathrm{VS}}]} \sim \left|\sigma^{(\mathrm{VS})} + j\omega\varepsilon_0\varepsilon_r^{(\mathrm{VS})}\right| \frac{[\Delta\phi_{\mathrm{VS}}]}{l_{\mathrm{VS}}}, \quad (2b)$$

$$\frac{[I]}{[A_{\mathrm{EL}}]} \sim \left|\sigma^{(\mathrm{EL})} + j\omega\varepsilon_0\varepsilon_r^{(\mathrm{EL})}\right| \frac{[\Delta\phi_{\mathrm{EL}}]}{l_{\mathrm{EL}}}, \quad (2c)$$

where $[I]$ is a scale for the absolute value of the total current passing through the skin, which has been estimated from the experimentally measured impedance, Z_{meas}, as $[I] \sim V_0/|Z_{meas}|$, $[A_{\mathrm{SC}}]$ is a scale for the area of the stratum corneum underneath the electrode, $[A_{\mathrm{VS}}]$ is a scale for the area that the current has to pass through in the radial direction in the viable skin, $[A_{\mathrm{EL}}]$ is a scale for the area of an electrode in contact with the skin; $[\Delta\phi_{\mathrm{VS}}]$, $[\Delta\phi_{\mathrm{EL}}]$ and $[\Delta\phi_{\mathrm{SC}}]$ are the scales of the absolute values of the potential drop in the viable skin, electrodes and stratum corneum, respectively; and l_{VS}, l_{EL} and l_{SC} are length scales in the radial direction in the viable skin and in the z-direction in the electrodes and stratum corneum. Typical values for these at 1 kHz are as follows: $l_{\mathrm{VS}} \sim 10^{-3}$ m, $l_{\mathrm{EL}} \sim 10^{-4}$ m, $l_{\mathrm{SC}} \sim 10^{-5}$ m, $[A_{\mathrm{VS}}] \sim 2\pi l_{\mathrm{VS}} h_{\mathrm{VS}} \sim 10^{-5}$ m^2, $A_{\mathrm{EL}} \sim \pi w_1^2 \sim 10^{-6}$ m^2, $A_{\mathrm{SC}} \sim A_{\mathrm{EL}}$, $\sigma^{(\mathrm{VS})} \sim 1$ S m^{-1}, $\sigma^{(\mathrm{EL})} \sim 10^7$ S m^{-1}, $\sigma^{(\mathrm{SC})} \sim 10^{-6}$ S m^{-1}, $\omega = 2\pi\nu \sim 10^4$ Hz, $\varepsilon_0 \sim 10^{-11}$ F m^{-1}, $\varepsilon_r^{(\mathrm{VS})} \sim 10^6$, $\varepsilon_r^{(\mathrm{EL})} \sim 1, \varepsilon_r^{(\mathrm{SC})} \sim 10^2$, and $[I] \sim 10^{-7}$ A for $V_0 = 0.05$ V. Here, we have approximated the scale for the areas of the electrodes with the area of the innermost electrode; the scale for the viable skin has been approximated as the area of the cylinder that the current has to pass through on its way through the viable skin from the injects to the sense electrode. In addition, we have used that the conductivity of layer i can be defined as follows: $\sigma^{(i)} = 1/\rho^{(i)}(\Omega)$.

With these values, we find

$$[\Delta\phi_{\mathrm{SC}}] \sim 0.05 \text{ V} \sim V_0,$$
$$[\Delta\phi_{\mathrm{VS}}] \sim 10^{-5} \text{ V},$$
$$[\Delta\phi_{\mathrm{EL}}] \sim 10^{-13} \text{ V}.$$

Clearly, $[\Delta\phi_{\mathrm{VS}}], [\Delta\phi_{\mathrm{EL}}] \ll [\Delta\phi_{\mathrm{SC}}]$. This, in turn, implies that we only need to consider the current passing through the stratum corneum underneath each electrode at frequencies around 1 kHz.

At this stage, it is also instructive to see how the potential drops distribute themselves at the other end of the frequency spectrum of the SciBase II probe: 1 MHz. Returning to the order-of-magnitude equivalents, Eqs. 2a-2c, and employing the typical magnitudes for the electrical parameters at 1 MHz, we obtain

$$[\Delta\phi_{\mathrm{SC}}] \sim 0.05 \text{ V},$$
$$[\Delta\phi_{\mathrm{VS}}] \sim 0.02 \text{ V},$$
$$[\Delta\phi_{\mathrm{EL}}] \sim 10^{-10} \text{ V}.$$

We have here used that $[I] \sim 10^{-4}$ A from the numerical solution of the full model (see *Numerics*) since a significant portion of the total current will pass through the guard, whence Z_{meas} at this high frequency does not capture the scale of the total current; $\sigma^{(\mathrm{VS})} \sim 1$ S m^{-1}, $\sigma^{(\mathrm{SC})} \sim 10^{-3}$ S m^{-1}, $\varepsilon_r^{(\mathrm{VS})} \sim 10^2$, $\varepsilon_r^{(\mathrm{SC})} \sim 10^2$ (the other parameters remain the same). In this limit, the viable skin is thus contributing significantly to the measured impedance.

Analytical solutions

In view of the findings at the lower limit of 1 kHz, for which the impedance of the skin is governed at leading order by the stratum corneum, we should be able to reduce the considered domain comprising three skin layers, the electrodes and the alternating current passing through them to a simple case of currents orthogonal to the electrodes passing in and out through the stratum corneum. Those currents would in turn give rise to the leading-order potential drop. From the mathematical point of view, it should thus be possible to reduce the partial differential equation to either ordinary differential or algebraic equations. We aim for the latter and proceed with the following Ansatz:

$$\sum_{k=1}^{4} I_k = 0, \quad (3a)$$

$$\frac{I_k}{A_k} = -(\sigma^{(\mathrm{SC})} + j\omega\varepsilon_0\varepsilon_r^{(\mathrm{SC})})\frac{\Delta\phi_k}{h_{\mathrm{SC}}}, \quad (3b)$$

$$\Delta\phi_1 = 0 - (V_0 - \Delta\phi_4), \quad (3c)$$

$$\Delta\phi_2 = 0 - (V_0 - \Delta\phi_4), \quad (3d)$$

j	$\mathfrak{c}_j^{(SC)}$	$\mathfrak{c}_j^{(VS)}$	$\mathfrak{c}_j^{(AT)}$	$\mathfrak{d}_j^{(SC)}$	$\mathfrak{d}_j^{(VS)}$	$\mathfrak{d}_j^{(AT)}$
0	-1.1803×10^{1}	2.3688×10^{1}	1.7402×10^{0}	1.7570×10^{1}	6.7610×10^{1}	7.5844×10^{0}
1	2.1404×10^{1}	-2.7471×10^{1}	0	-1.7961×10^{1}	-7.0466×10^{1}	8.3142×10^{-2}
2	-9.9955×10^{0}	1.2952×10^{1}	0	8.5278×10^{0}	3.2847×10^{1}	-7.7214×10^{-1}
3	2.2537×10^{0}	-3.0088×10^{0}	0	-2.0255×10^{0}	-7.7649×10^{0}	1.1797×10^{-1}
4	-2.5509×10^{-1}	3.4167×10^{-1}	0	2.3953×10^{-1}	9.2429×10^{-1}	-4.0926×10^{-4}
5	1.1516×10^{-2}	-1.5178×10^{-2}	0	-1.1319×10^{-2}	-4.4465×10^{-2}	-5.2423×10^{-4}

Tab. 2: Cofficients for the material properties.

$$\Delta\phi_3 = \alpha V_0 - (V_0 - \Delta\phi_4). \tag{3e}$$

Here, $\Delta\phi_k$ and I_k are the potential drop and current through the stratum corneum underneath electrode k respectively, as illustrated in Fig. 1c; and h_{SC} is the height of the stratum corneum. The current passing through each electrode, I_k, is positive when coming out (positive z-direction in Fig. 1) and going into (negative z-direction) the skin respectively.

The area for each electrode, A_k, is given by

$$A_k = \pi \begin{cases} w_1^2, & k = 1, \\ w_{2k-1}^2 - \left(\sum_{k=1}^{2k-2} w_k\right)^2, & k = 2,3,4. \end{cases} \tag{3f}$$

In essence, Eq. 3a ensures that the total current is preserved, which can thus be seen as a representation of the conservation of charge, Eq. 1a; Eq. 3b is derived from the definition of the current density, **J**, in Eq. 1b, in which the gradient has been replaced with the potential drop and height of stratum corneum; and the potential drop for the three innermost electrodes – current detection ($k = 1$), guard ($k = 2$), and second injection electrode ($k = 3$) – in Eqs. 3c-3e over the stratum corneum underneath the electrodes originate from the boundary conditions, Eqs. 1c-1f.

We have thus reduced the complex-valued partial differential equation in the rotation-symmetric domain comprising stratum corneum, viable skin and adipose tissue together with constitutive relations and boundary conditions to a system of 8 linear algebraic equations with 8 unknowns: I_k and $\Delta\phi_k$ for $k = 1,..,4$. Note that the Ansatz can be adjusted to other probe designs, such as rectangular probes, or probes with more or less electrodes.

After some algebra, we arrive at the following closed-form expression for the electrode currents:

$$I_k = -A_k(\sigma^{(\mathrm{SC})} + j\omega\varepsilon_0\varepsilon_r^{(\mathrm{SC})})\frac{\Delta\phi_k}{h_{\mathrm{SC}}}, \tag{4a}$$

where

$$\Delta\phi_1 = V_0(\mathfrak{A} - 1), \tag{4b}$$
$$\Delta\phi_2 = V_0(\mathfrak{A} - 1), \tag{4c}$$
$$\Delta\phi_3 = V_0(\mathfrak{A} - 1 + \alpha), \tag{4d}$$
$$\Delta\phi_4 = V_0\mathfrak{A}, \tag{4e}$$

with the constant, $\mathfrak{A}$, given by

$$\mathfrak{A} = \frac{[A_1 + A_2 + A_3(1-\alpha)]}{A_1 + A_2 + A_3 + A_4}, \tag{4f}$$

which is the ratio of the areas of the three inner electrodes modified with the depth of the second injection electrode ($k = 3$) and the sum of the total electrode areas.

The impedance, Z, can then be evaluated from

$$Z = \frac{V_0}{I_1}, \tag{5}$$

where I_1 is the current passing through the sense electrode, resulting in

$$Z = \frac{h_{\mathrm{SC}}}{A_1(1-\mathfrak{A})(\sigma^{(\mathrm{SC})} + j\omega\varepsilon_0\varepsilon_r^{(\mathrm{SC})})}. \tag{6}$$

We will later analyze the findings from the impedance in the form of the magnitude, $\mathfrak{M}$, and the phase, $\mathfrak{P}$, which can be expressed as

$$\mathfrak{M} = \frac{h_{\mathrm{SC}}}{A_1(1-\mathfrak{A})\sqrt{\left(\sigma^{(\mathrm{SC})}\right)^2 + \left(\omega\varepsilon_0\varepsilon_r^{(\mathrm{SC})}\right)^2}}, \tag{7a}$$

$$\mathfrak{P} = \arctan\left(-\frac{\omega\varepsilon_0\varepsilon_r^{(\mathrm{SC})}}{\sigma^{(\mathrm{SC})}}\right) \times \frac{180\,^\circ}{\pi}. \tag{7b}$$

Finally, it is interesting to note that in the limit of 1 kHz the magnitude depends on the thickness of the stratum corneum, depth setting, frequency, material properties of stratum corneum, and the areas of the electrodes; whereas the phase is only a function of the frequency and material properties of the stratum corneum. Furthermore, both the magnitude and the phase are not functions of the applied voltage. This independence of the applied voltage has been confirmed by tests with the probe in the range from 50 mV to 250 mV, for which the measured impedance did not change at leading order (not shown here).

Electrical properties of the stratum corneum

So far, we have derived closed-form expressions for the currents, impedance, magnitude and phase at frequencies around 1 kHz. Now, if we have access to an experimentally measured impedance, Z_{meas}, we can inverse the expressions to estimate electrical properties – conductivity and relative permittivity – of the stratum corneum provided that the latter's thickness, h_{SC}, is known:

$$\sigma^{(\mathrm{SC})} = \frac{a h_{\mathrm{SC}}}{A_1(1-\mathfrak{A})(a^2+b^2)}, \tag{8a}$$

$$\varepsilon_r^{(\mathrm{SC})} = -\frac{b h_{\mathrm{SC}}}{A_1(1-\mathfrak{A})(a^2+b^2)\omega\varepsilon_0}; \tag{8b}$$

here, $a = \mathrm{Re}(Z_{meas})$ and $b = \mathrm{Im}(Z_{meas})$. (*N.B.*: $b \leq 0$.)

Stratum corneum thickness

If either the relative permittivity and/or the conductivity is known, then we are able to estimate the thickness of the stratum corneum, after some algebra, from either the imaginary part of the measured impedance

$$h_{\mathrm{SC}} = -\frac{\varepsilon_r^{(\mathrm{SC})}\varepsilon_0\omega A_1(1-\mathfrak{A})(a^2+b^2)}{b}, \tag{9a}$$

or the real part

$$h_{\mathrm{SC}} = \frac{\sigma^{(\mathrm{SC})}A_1(1-\mathfrak{A})(a^2+b^2)}{a}, \tag{9b}$$

or as an average of the two

$$h_{\mathrm{SC}} = \frac{A_1(1-\mathfrak{A})(a^2+b^2)}{2}\left(\frac{\sigma^{(\mathrm{SC})}}{a} - \frac{\varepsilon_r^{(\mathrm{SC})}\varepsilon_0\omega}{b}\right). \tag{9c}$$

Numerics

For verification of the analytical solution in the limit of low frequencies ($\nu \sim 1$ kHz) and the region of validity, the mathematical model, Eqs. 1a-1i, was also implemented and solved in the commercial finite-element solver, COMSOL MULTIPHYSICS 3.5a [20]. In this context, verification refers to ensuring that we have not unwittingly discarded any leading-order terms (read: significant terms) when reducing the full set of equations to a simple algebraic counterpart.

In essence, the computational domain shown in Fig. 1 was resolved with a mesh of around 10^5 triangular elements after a mesh-independence study to ensure mesh-independent results; the direct solver PARDISO was selected as the linear solver with a relative convergence tolerance of 10^{-6}.

A typical run required around 2 seconds (wall-clock time) with 5×10^4 degrees of freedom (quadratic Lagrange elements) on a 2.5 GHz workstation for a given frequency.

Results and discussion

We have thus far outlined the methods and materials that we intend to employ in order to estimate the thickness and electrical properties of the stratum corneum from EIS measurements. Before attempting those estimates, we need to verify the analytical solutions in the limit of 1 kHz and explore their region of validity; i.e., for which range of frequencies the solutions are reasonably valid. After verification, we proceed with the experimental measurements at various depth settings for further validation of the underlying mathematical formulation. Finally, we attempt to determine the material properties – resistivity and relative permittivity – as well as the stratum corneum thickness from the experimental impedance measurements.

Verification

In order to verify the analytical solutions and establish their region of validity, we compare the predicted magnitude and phase with their counterparts from the full set of equations, Eqs. 1a-1i, through the frequency range 1-10^3 kHz. As can be inferred from Fig. 2, the analytical solutions are able to predict the magnitude and phase of the EIS in the low to mid-frequency range up to around 10^2 kHz with an error less than 10%; after 10^2 kHz, the error increases rapidly up to around 25% and 40% for the magnitude and phase respectively.

The main causes for the increasing error with increasing frequency can be found in the underlying assumptions of the Ansatz: first, the assumption that the electrical impedance is dominated by the stratum corneum whilst the viable skin and subcutaneous fat are negligible becomes less accurate with increasing frequency, because it is well known that the impedance of the skin is governed by the stratum corneum only at lower frequencies whilst its influence decreases when the frequency increases [18, 19]; this was also demonstrated in the earlier scaling analysis. Second, the assumption that the currents pass straight through the stratum corneum is reasonable in the low- to mid-frequency range; at higher frequencies, however, the current density distributions underneath the electrodes becomes increasingly more non-uniform and thereby alter the active area of the electrodes (A_{1-4}). Third, the assumption that the voltage drop will not occur solely over the stratum corneum becomes less accurate with increasing frequency, as was shown earlier with the scales for the potential drops in the scaling analysis around 10^3 kHz.

Proceeding with verifying the individual currents for each electrode, as depicted in Fig. 3, we find that the real part agrees well throughout the frequency range, whereas the imaginary part starts to deviate above the earlier observed 10^2 kHz.

One of the reasons for the good agreement of the real part, $\mathrm{Re}(I_k) = -A_k\sigma\Delta\phi_k/h_{SC}$, as opposed to imaginary part of the current, $\mathrm{Im}(I_k) = -A_k\omega\varepsilon_0\varepsilon_r\Delta\phi_k/h_{SC}$, could be that the latter has an explicit dependence on ν ($\omega = 2\pi\nu$), which increases by three orders of magnitude from 1 to 10^3 kHz; this, in turn, affects the error propagation as the frequency increases. Nonetheless, the region of validity of the analytical solutions extends by two orders of magnitude beyond 1 kHz to around 10^2 kHz compared to the numerical solution of the full set of equations, which is in line with our earlier intuition regarding the extent of the region of validity.

Validation

So far, we have verified and determined the region of validity of our Ansatz and resulting analytical closed-form expressions for the impedance measured during EIS of skin. We will now seek to further validate the mathematical model – solved numerically and analytically – by exploiting the different depth settings of the probe.

The measurements were carried out at five different depth settings, $\alpha_n = (0.1, 0.27, 0.58, 0.81, 1)$ as shown in Fig. 4

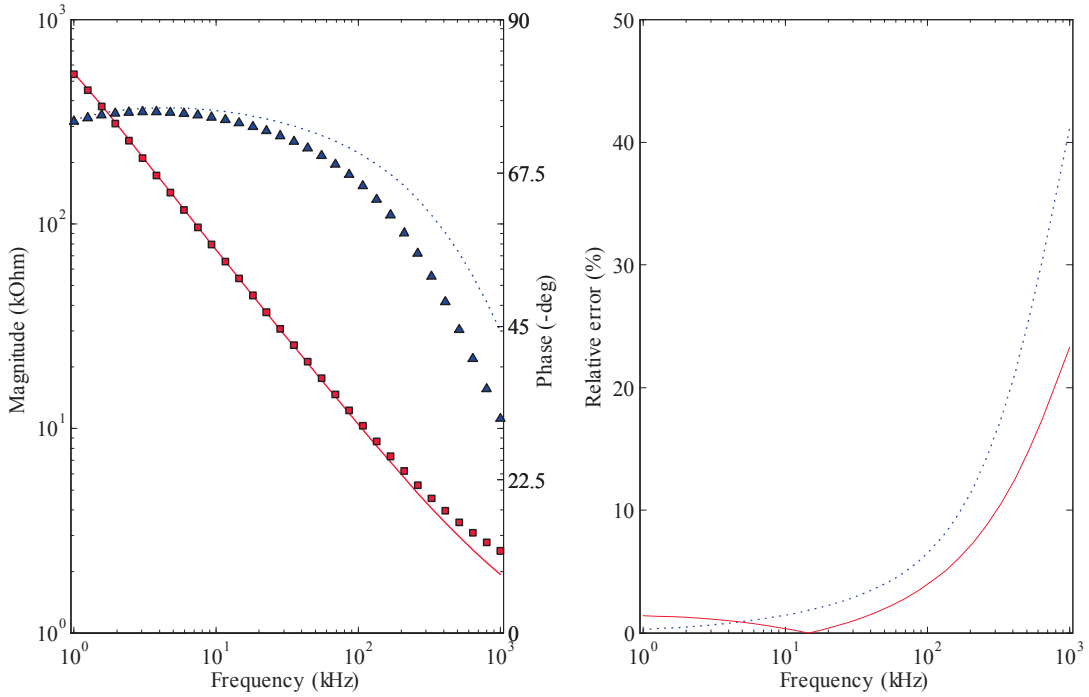

Fig. 2: (a) The magnitude (■) and phase (▼) from the numerical solution of the full set of equations and the analytical counterparts (lines); (b) the relative error for the analytical solution relative to the full set of equations for the magnitude (—) and phase (- - -).

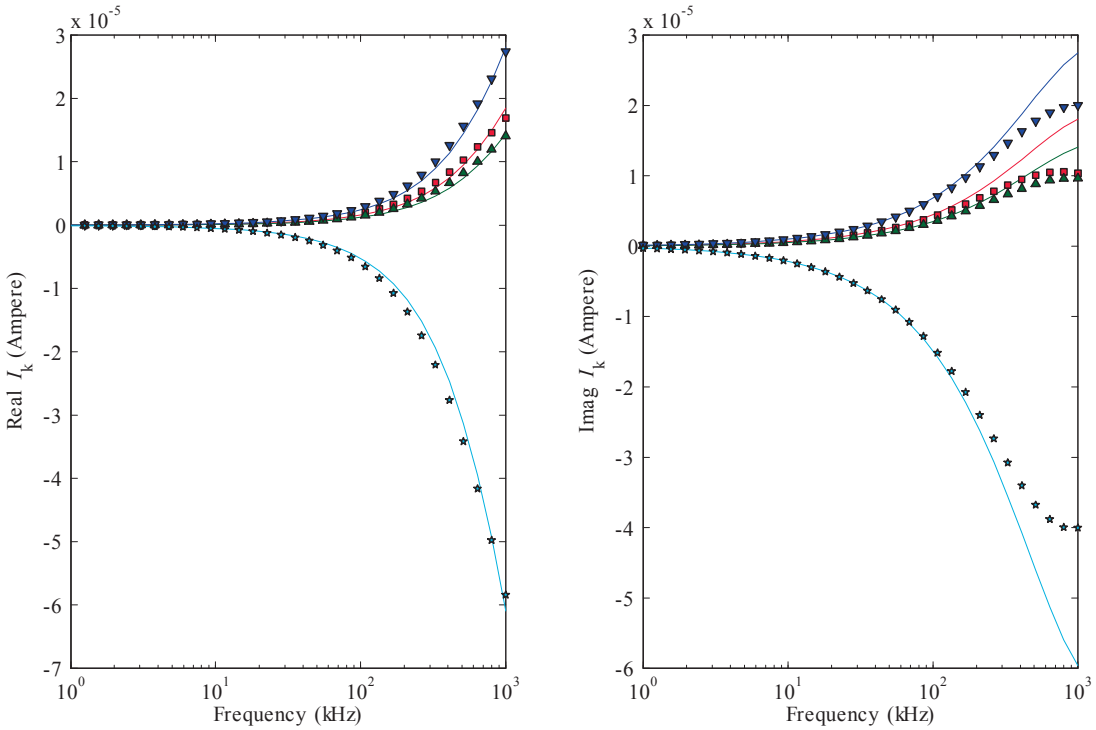

Fig. 3: The individual currents, I_k, in terms of their (a) real and (b) imaginary parts for the numerical solution of the full set of equations (symbols) and the analytical counterpart (lines); here, (★) I4,(▲) I2, (■) I1, and (▼) I3.

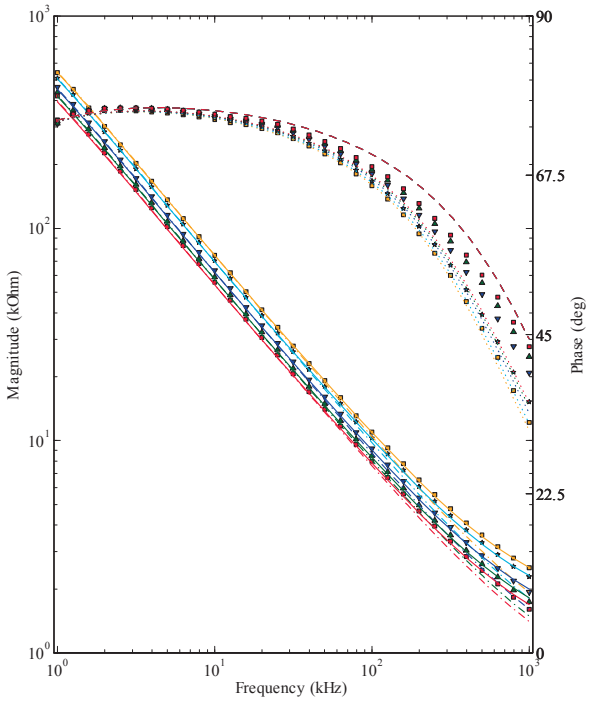

Fig. 4: Magnitude and phase of the of the numerical solution (...), analytical solution (−−) and the experimental data (symbols) at five depth settings α_n= (■ 0.1, ▲ 0.27, ▼0.58, ★ 0.81, ■ 1).

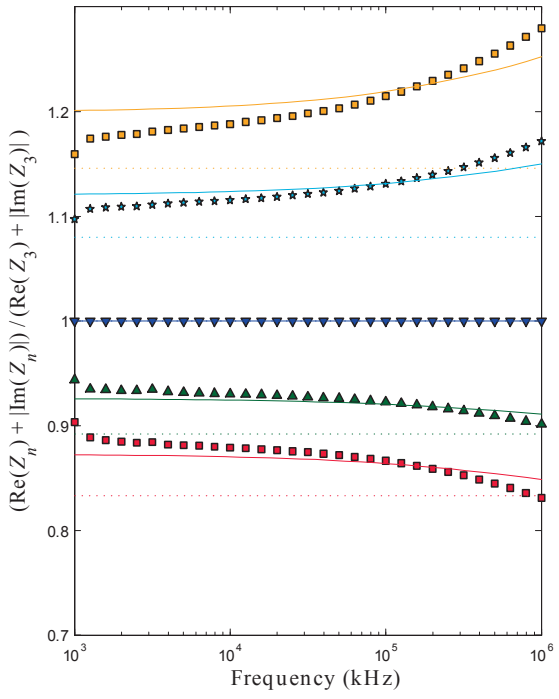

Fig. 5: The ratio of the impedance to the numerical solution (...), analytical solution (−−) and the experimental data (symbols) at five depth settings α_n= (■ 0.1, ▲ 0.27, ▼ 0.58, ★ 0.81, ■ 1).

for the magnitude and the phase from the experimental measurements and predictions from the full model and analytical expressions. Here, several features are apparent: first and foremost is the good agreement between the predicted magnitude and phase for the depth setting, $\alpha = 0.1$, which is due to the calibration of the conductivity and relative permittivity at this depth (see [17]); second is that the numerical solution of the full set of equations is not fully able to capture the shift in the phase as the frequency approaches 10^3 kHz, although its magnitude adheres closely to the measured counterpart; third, and as expected, is that the closed-form expressions are limited to a region between 1 and 10^2 kHz in their validity; and fourth, is that the measured phase at different depth settings converges towards a single value for $\nu \longrightarrow 1$ kHz, supporting the closed-form expression for the phase, Eq. 7b, which does not contain the depth, as opposed to the closed-form solution for the magnitude, Eq. 7a.

Returning to the analytical solution for the impedance, Eq. 6, and extending it for different depth settings as

$$Z_n = \frac{h_{\mathrm{SC}}}{A_1(1-\mathfrak{A}_n)(\sigma^{(\mathrm{SC})} + j\omega\varepsilon_0\varepsilon_r^{(\mathrm{SC})})}, \tag{10a}$$

$$\mathfrak{A}_n = \frac{[A_1 + A_2 + A_3(1-\alpha_n)]}{A_1 + A_2 + A_3 + A_4}, \tag{10b}$$

we find that the depth settings and their impact reduce to a constant by taking the ratio of impedances at different depth settings:

$$\frac{Z_n}{Z_3} = \frac{1-\mathfrak{A}_3}{1-\mathfrak{A}_n} = \text{constant},$$

which agrees well with the corresponding experimentally measured impedance ratios at 1 kHz and numerical and analytical counterpart, as can be inferred from Fig. 5. The maximum relative error between the measured and predicted ratios varies between 0 and 8 %. In addition, it is likely that the experimental measurements are imprecise around 1 kHz, since there is no physical justification for the ratios to suddenly change abruptly when $\nu \rightarrow 1$ kHz.

A closer look at the individual currents (not shown here) reveals that the current changes direction at the second injection electrode ($k = 3$) for $\alpha_{4,5}$ since the applied voltage there is now 58% and 100% of the voltage at the primary injection electrode ($k = 4$). This demonstrates that the Ansatz is able to capture the dual role of the second injection electrode to act akin to a guard at low depths and as an inject at higher depth settings. In fact, a closer inspection of Eq. 4d reveals that $\Delta\phi_3$ changes sign when $\alpha = 1 - \mathfrak{A}$.

Electrical properties

From Eqs. 8a and 8b as well as by assuming the stratum corneum thickness to be 14 μm, we are able to estimate the resistivity and the relative permittivity for each individual subject separately. As can be inferred from Fig. 6, the closed-form analytical expressions follow the numerical counterparts up to around 10^2 kHz, after which the relative permittivity starts to deviate whilst the resistivity agrees throughout the frequency range.

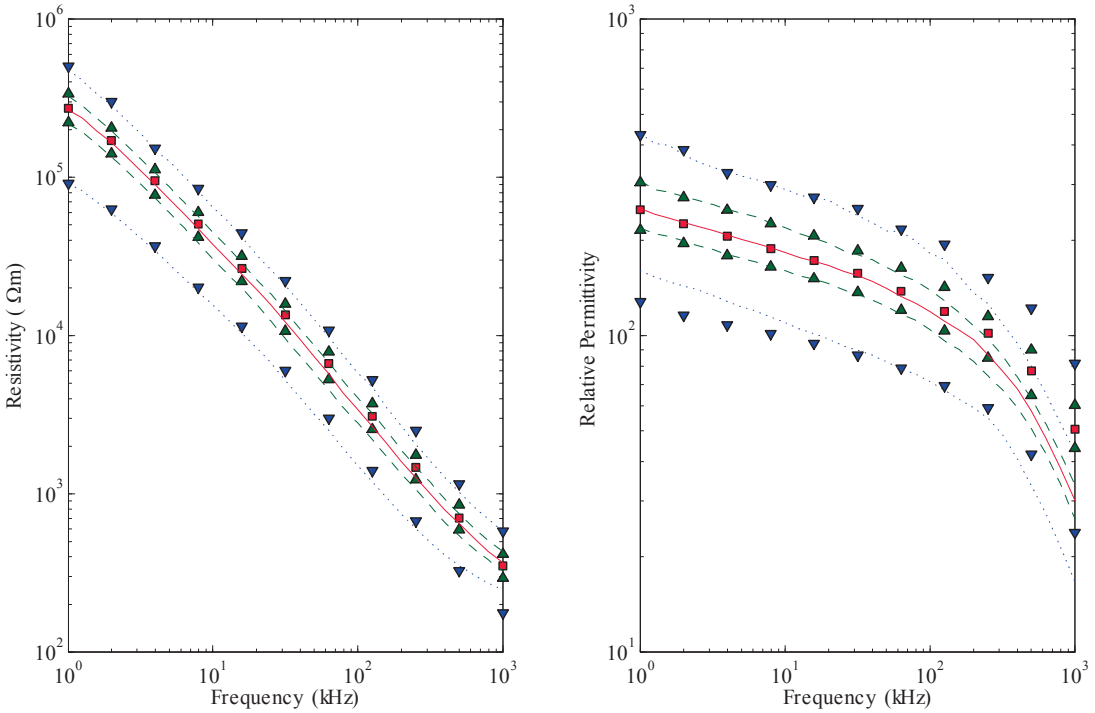

Fig. 6: The median predicted (a) resistivity and (b) relative permittivity for the full set of equations (■) with ±1 standard deviation (▲), ±2 standard deviations (▼) and the closed-form expressions (−) with ±1 standard deviation (−−), ±2 standard deviations (...).

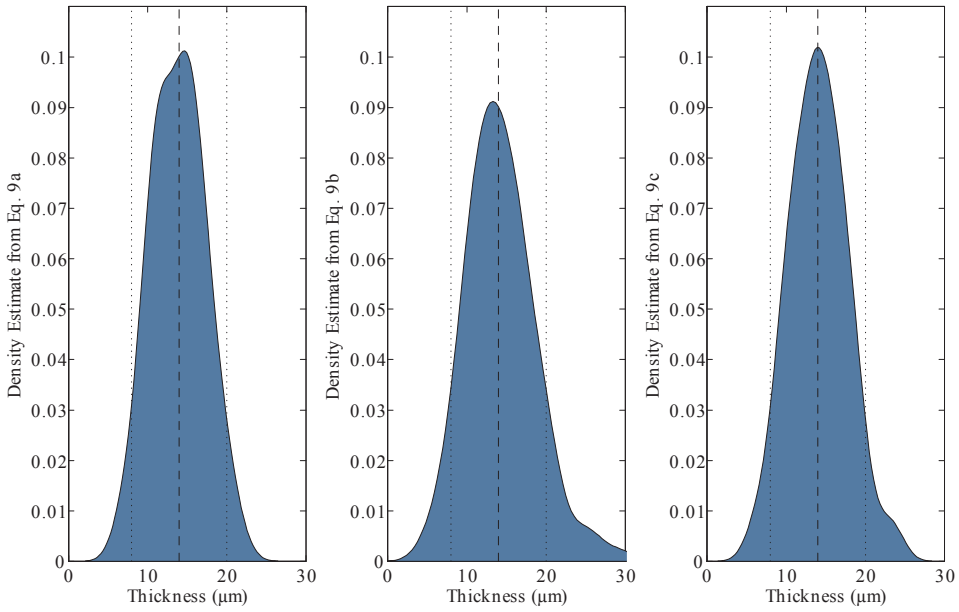

Fig. 7: The estimated thickness distributions for stratum corneum based on the real and imaginary part from EIS measurements and a combination of the two.

We recall that the resistivity captures more information of the real part of the impedance, a, whilst the relative permittivity, as previously noted, has an explicit dependence on ω and includes more information of the imaginary part, b. Clearly, the same phenomenon observed for the real and imaginary part of the current in the analytical solution carries through for the estimates of the electrical properties. We therefore once more find that the region of validity extends beyond 1 kHz to around 10^2 kHz**.**

Stratum corneum thickness

Finally, we estimate the thickness of the stratum corneum with Eqs. 9a-9c by assuming that the material properties are known. As illustrated in Fig. 7, the stratum corneum thickness estimate based on the real part of the impedance overestimates the skin thickness slightly, whilst the imaginary part underestimates the skin thickness somewhat; their combination, however, gives rise to an accurate distribution with 92% of the individuals between 6 and 20 μm, which corresponds well with literature values [8]. These findings suggest that one should thus employ both the real and imaginary parts of the measured impedance to ensure as accurate estimates as possible – this makes sense since we are tapping into more information from the EIS by including both contributions.

At this stage, it would have been useful to have access to other types of measurements of the stratum corneum thickness of the 120 subjects to further provide evidence of the fidelity of the predictions. This is especially the case since we have taken material properties that were calibrated for a median skin thickness of 14 μm.

Conclusions

A mathematical model for EIS of skin has been analyzed and closed-form analytical expressions have been derived in the limit of low frequencies around 1 kHz. Their accuracy and region of validity were found to be 1 kHz to around 10^2 kHz from the verification of the full set of equations solved numerically as well as validation with experimentally measured impedances at different depth settings from a total of 120 subjects.

In summary, the analytical expressions were found from scaling analysis and a subsequent Ansatz that reduced the full set of equations – one complex partial differential equation with constitutive relations and boundary conditions in the stratum corneum, viable skin and adipose tissue – to a set of algebraic equations. The latter were solved, resulting in closed-form analytical expressions for the electrical impedance, magnitude, phase, electrical properties as well as the thickness of stratum corneum.

By combining experimental impedance measurements with the analytical expressions, we were able to not only estimate the electrical properties of the stratum corneum (provided the stratum corneum thickness is known) but also its thickness. The latter was carried out for all 120 subjects in the study, resulting in a stratum corneum thickness distribution with a mean of 14 μm with standard deviation $\pm$3.6 μm, which is in line with reported literature values for the stratum corneum thickness distribution. This suggests that EIS could be employed as a method to estimate the stratum corneum thickness at 1 kHz; its suitability could be further validated by carrying out EIS measurements in tandem with one or several of the aforementioned techniques to measure the stratum corneum thickness (see *Introduction)* to establish that one is indeed measuring a reasonably "true" thickness of the stratum corneum for each subject and not just the distribution.

References

1. M. Egawa, H. Tagami. Comparison of the depth profiles of water and water-binding substances in the stratum corneum determined in vivo by raman spectroscopy between the cheek and volar forearm skin: effects of age, seasonal changes and artificial forced hydration. Br J Dermatol. 2008;158:251-260. http://dx.doi.org/10.1111/j.1365-2133.2007.08311.x
2. J. M. Crowther, A. Sieg, P. Blenkiron, C. Marcott, P. J. Matts, J. R. Kaczvinsky, A. V. Rawlings. Measuring the effects of topical moisturizers on changes in stratum corneum thickness, water gradients and hydration in vivo. Br J Dermatol. 2008;159:567–577. http://dx.doi.org/10.1111/j.1365-2133.2008.08703.x
3. M. Huzaira, F. Rius, M. Rajadhyaksha, R. R. Anderson, S. Gonzáles. Topographic variations in normal skin, as viewed by in vivo reflectance confocal microscopy. J Invest Dermatol. 2001;116:846-852. http://dx.doi.org/10.1046/j.0022-202x.2001.01337.x
4. T. L. Moore, M. Lunt, B. McManus, M. E. Anderson, A. L. Herrick. Seventeen-point dermal ultrasound scoring system-a reliable measure of skin thickness in patients with systemic sclerosis. Rheumatology 2003;42:1559-1563. http://dx.doi.org/10.1093/rheumatology/keg435
5. J. Sandby-Moller, T. Poulsen, H. C. Wulf. Epidermal thickness at different body sites: relationship to age, gender, pigmentation, blood content, skin type and smoking habits. Acta Derm Venereol. 2003;83:410-413. http://dx.doi.org/10.1080/00015550310015419
6. K. Holbrook, G. Odland. Regional differences in the thickness (cell layers) of the human stratum corneum: An ultrastructral analysis. J Invest Dermatol. 1974;62:415-422. http://dx.doi.org/10.1111/1523-1747.ep12701670
7. D. A. Schwindt, K. P. Wilhelm, H. I. Maibach. Water diffusion characteristics of human stratum corneum at different anatomical sites in vivo. J Invest Dermatol. 1998;111:385-389. http://dx.doi.org/10.1046/j.1523-1747.1998.00321.x
8. U. Birgersson, E. Birgersson, P. Åberg, I. Nicander, S. Ollmar. Non-invasive bioimpedance of intact skin: mathematical modeling and experiments. Physiol. Meas. 2011;32:1-18. http://dx.doi.org/10.1088/0967-3334/32/1/001
9. Walker D C, Brown B H, Smallwood R H, Hose D R, Jones D M. Modelled current distribution in cervical squamous. Physiol. Meas. 2002;23:159-68. http://dx.doi.org/10.1088/0967-3334/23/1/315

10. Jones D M, Smallwood R H, Hose D R, Brown B H, Walker D C. Modelling of epithelial tissue impedance measured using three different design of probe. Physiol. Meas. 2003;24:605-23. http://dx.doi.org/10.1088/0967-3334/24/2/369
11. Walker D C, Brown B H, Blackett A D, Tidy J, Smallwood R H. A study of the morphological parameters of cervical squamous epithelium. Physiol. Meas. 2003;24:121-35. http://dx.doi.org/10.1088/0967-3334/24/1/309
12. Walker D C, Brown B H, Smallwood R H, Hose D R, Jones D M. Modelling the electrical properties of bladder tissue–quantifying impedance changes due to inflammation and oedema. Physiol. Meas. 2005;26:251-68. http://dx.doi.org/10.1088/0967-3334/26/3/010
13. Keshtkar A, Keshtkar A, Smallwood R H. Electrical impedance spectroscopy and the diagnosis of bladder pathology. Physiol. Meas. 2006;27:586-96. http://dx.doi.org/10.1088/0967-3334/27/7/003
14. Hartinger A E, Guardo R, Kokta V, Gagnon H. A 3D hybrid finite element model to characterize the electrical behavior of cutaneous tissues. IEEE Trans. Biomed. Eng. 2010;57:780-9. http://dx.doi.org/10.1109/TBME.2009.2036371
15. SciBase, Scibase ab homepage, http://www.scibase.se.
16. Åberg P. Skin cancer as seen by electrical impedance PhD thesis Karolinska Institutet. Stockholm, Sweden. 2004.
17. U. Birgersson, E. Birgersson, S. Ollmar. A methodology for extracting the electrical properties of human skin. Manuscript submitted for publication in Physiol. Meas. 2012.
18. J. J. Ackmann, M. A. Seitz. Methods of complex impedance measurements in biologic tissue. Crit Rev Biomed Eng. 1984;11:281-311.
19. O. G. Martinsen, S. Grimnes, E. Haug. Measuring depth depends on frequency in electrical skin impedance measurements. Skin Res Technol. 1999;5:179-181. http://dx.doi.org/10.1111/j.1600-0846.1999.tb00128.x
20. COMSOL, Multiphysics Multiphysics 3.5a, http://www.comsol.com.